Iorio, M., Santarelli, M. L., González-Gaitano, G., & González-Benito, J. (2018). Surface modification and characterization of basalt fibers as potential reinforcement of concretes. Applied Surface Science, 427, 1248-1256.

doi:https://doi.org/10.1016/j.apsusc.2017.08.196

Graphical Abstract (for review)

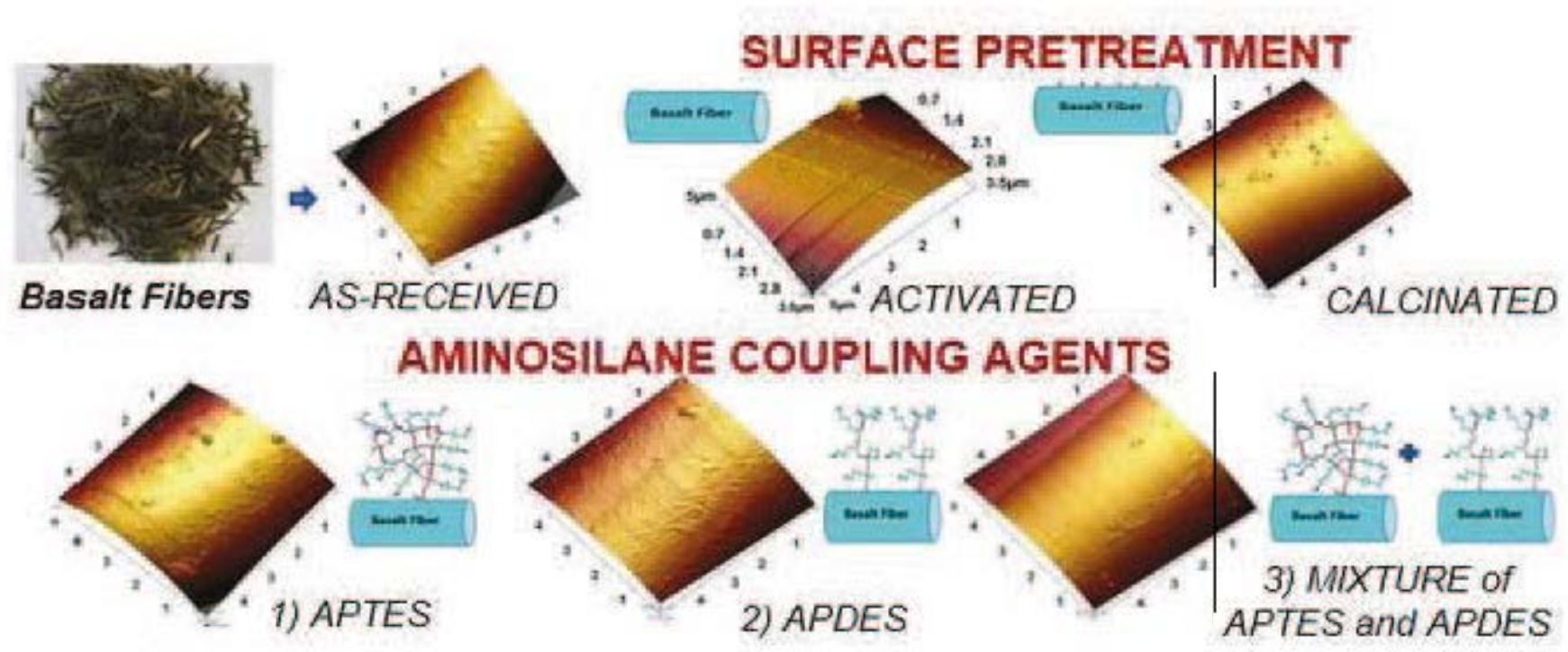

Surface Modification and Characterization of Basalt Fibers as Potential Reinforcement of Concretes

M. Iorio[1,2], M.L. Santarelli[2,3], G. González-Gaitano[4], J. González-Benito [1*]

[1]Universidad Carlos III de Madrid, Departamento de Ciencia e Ingeniería de Materiales e Ingeniería Química, IQMAAB, Av.da de la Universidad 30, 28911 Leganés, Spain.

[2]Sapienza-Università di Roma, Dipartimento di Ingegneria Chimica Materiali Ambiente. Via Eudossiana 18, 00184 Rome, Italy.

[3]CISTEC-Centro di Ricerca in Scienza e Tecnica per la conservazione del patrimonio storico-architettonico, Via Eudossiana 18, 00184 Rome, Italy.

[4]Universidad de Navarra, Departamento de Química, Facultad de Ciencias, C/ Irunlarrea, 31008 Pamplona, Spain.

[*] Corresponding author at: Universidad Carlos III de Madrid, Departamento de Ciencia e Ingeniería de Materiales e Ingeniería Química, IQMAAB, Escuela Politécnica Superior, Av.da de la Universidad nº 30, 28911 Leganés (Madrid), Spain.
E-mail address: javid@ing.uc3m.es
Telephone number: +34 91 624 88 70

Abstract

Basalt fibers were surface treated with silane coupling agents as a method to enhance the adhesion and durability of fiber-matrix interfaces in concrete based composite materials. In particular, this work has been focused on the study of basalt fibers chemical coatings with aminosilanes and their subsequent characterization. Surface treatments were carried out after removing the original sizing applied by manufacturer and pretreating them with an activation process of surface silanol regeneration. Different samples were considered to make convenient comparisons: as received fibers (commercial), calcinated fibers (without

commercial sizing), activated samples (calcinated fibers subjected to an acid process for hydroxyl regeneration), and silanized fibers with *γ-aminopropiltriethoxysilane, γ-aminopropilmethyldiethoxysilane* and a mixture of 50% by weight of both silanes. A deep characterization was carried out in terms of structure using X-ray diffraction, XRD, and Fourier transform infrared spectroscopy, FTIR, thermal properties by thermogravimetric analysis, TGA, coupled with single differential thermal analysis, SDTA, and morphology by scanning electron microscopy, SEM, and atomic force microscopy, AFM.

Keywords:

Basalt fibers, surface treatments, silane coupling agents

1. INTRODUCTION

Nowadays, several industrial applications require the use of new low cost and environmental friendly materials. Among others, one of the possible strategies to overcome the later may be the use of composite materials looking for the most efficient sinergy between the constituents. In this context the design of fiber-reinforced composite materials is especially interesting, being probably the use of natural fibers one of the most important reinforcing element to be considered. Among them, basalt fibers extruded from naturally fire-resistant basalt represent a very promising reinforcing agent for this type of materials [1,2]. The chemical composition of basalt fiber is closely similar to a common syntetic glass fiber. Its basic components are SiO_2 (the main constituent), Al_2O_3, CaO, MgO, K_2O, Na_2O, Fe_2O_3 and FeO [3,4].

The choice of basalt fibres lies in the fact that they are characterized from a large variety of excellent properties such as high tensile strength, high E-modulus, high abrasion strength, high temperature resistance, high resistance to aggressive media, excellent thermal and sound insulation, good chemical stability [5]. Thus, in many cases basalt fibers might be an extraordinary candidate to replace synthetic fibers as glass and carbon fibers in composite materials. Besides, basalt fibers have better tensile strength than the E-glass fibers, greater failure strain than carbon fibers as well as good resistance to chemical attack. Therefore, the potentiality of basalt fibers as structural strengthening material is evident [6].

Moreover, basalt fibers can be easily processed using conventional methods and equipments and they do not need any other additional step in the single producing process, making them to have an additional advantage in terms of costs [7]. Finally, it is interesting to highlight that basalt fibers are safe for health because their diameters are larger than 9 micrometers and they are not subjected to longitudinal fracture so they cannot be considered as inhalable materials. Due to the last characteristics basalt fibers have been recently classified as *"The green*

industrial material for the twenty-first century" [8]. This definition reveals the sustainability, point of growing interest in new worldwide productions.

One of the final use of fibers is as reinforcement of concrete in structural materials to reduce the adverse effects of shrinkage cracking of cement and natural hydraulic lime (NHL) mortars used in many historical structures and buildings which have significant cultural interest.

Most of the restoration interventions have employed cement-based mortars that have shown several incompatibilities (high mechanical strength, efflorescence phenomena owing to the formation of large amounts of soluble salts by migrations of alkaline ions, low permeability with excessive water retention) causing extensive damage to the ancient masonry. Due to these problems, the last years have been focused on using lime-based mortars for restoration activities, looking for higher compatibility (physical, chemical and mechanical) between the new repair mortar and original components [9,10].

Sarasini et al. in 2014 [9,10] investigated the effect of commercial basalt fibers in this type of matrices studying the mechanical properties in terms of fracture and damage mechanism highlighting the role played by the interface between the fiber and the cement matrices. However, they pointed out the necessity of carrying out more investigation focused on this issue trying to find out how inducing a better balance between two usually opposing needs, strength and toughness enhancement.

It is well known that properties of composite materials are strongly influenced by the type of adhesion between the reinforcement and the matrix [11,12]. Depending on the characteristics of the fiber-matrix interfacial region, the composite subjected to different sorts of loads can be either brittle or damage-tolerant under the effect of several factors or even combination of them (temperature, radiation, humidity). Thus, in order to obtain composites with good mechanical properties it is important, among other things, to tailor a proper fiber-matrix interface to improve final performance of the composites avoiding, for instance, several

failure mechanisms that could start at the interface such as fiber debonding and pull-out, fiber sliding and crack bridging [13].

The surface modification of reinforcements trough especial treatments is one of the most common strategies to overcome the later. Probably the most successful method to carry out this lies on the creation or increment of particular functional groups to facilitate physical interactions or even chemical bonding between the constituents [14]. Therefore, it is reasonable to think that also, in the case of basalt fibers, one of the challenges must be optimizing the fiber-matrix interface through surface treatments of the fibers to finally increase the attractive interactions, reduce imperfections and, protect the fibers from the aggressive environment given by the matrix. The usual way to fulfill the later is by generating: i) an adequate roughness, for instance, to increase the specific surface and ii) a surface with particular chemical functionalities.

It is well known that coupling agents have a great effect on the interface structure and properties of composite materials [12,15]. Among them, the most commonly used are those called silane coupling agents consisting on difunctional organosilicon compounds, one, -X, compatible or chemically reactive with the reinforcement and, the other, -Y compatible or chemically reactive with the matrix. They usually have the general formula $Y\text{-}Si(X)_3$, where X represents a hydrolizable group (such as methoxy, ethoxy or chlorine) which after hydrolyzing to silanol, can react with silanol groups present on the surface of basalt fiber to form siloxane linkages, and Y represents a nonhdrolyzable organanofunctional group such amino, mercapto, epoxy, etc. group physically or chemically compatible with the matrix [14]. In particular, aminosilanes are commonly used as surface modifying agents in fibers [14,16–29]. Besides, several studies shown that they can improve the composite performance in several matrices (as cement matrix) [30,31]. When modifying with this kind of silanes special attention must be paid on the interphase structure since it is quite well known that, because of the chemical and structural differences of this coupling agent interface layer can greatly

influence in the mechanical properties of composite materials [14]. Thus, a good characterization of fibers surface along the whole process of their modification is a prerequisite to finally understand the last properties of the composites.

The aim of this work is to modify basalt fibers surface under well controlled conditions using different model surface treatments and characterize them in such a way that the data collected (structure, morphology, etc.) were enough to finally understand possible improvements of the properties of cement based composite materials. The surface treatments will be based on chemical coatings of the basalt fiber with aminosilanes having different functionally order (triethoxysilane, 3, diethoxysilane, 2, and a mixture of them 50% by weight). These choices were made looking for obtaining different molecular structure at the fiber surface and consequently at the interface of composites.

2. EXPERIMENTAL

2.1 Materials

Basalt continuous filament (mean diameter 17 μm) chopped to a length of about 6.4 mm with a sizing compatible with cement and natural hydraulic lime (NHL) matrices was supplied by Incothelogy GmbH. Two silanes, γ-aminopropiltriethoxysilane (APTES) and γ-aminopropilmethyldiethoxysilane (APDES), supplied by ABCR GmbH & Co.KG, were used in order to obtain different surface coatings of the basalt fibers.

2.2 Sample Preparation

Neat basalt fibers were obtained by a surface pretreatment of the as-received fibers following several steps:

- ✓ Disgregation: Commercial basalt fibers were initially stirred within destilled and deionized water at room temperature to attain maximum separation between them.

- ✓ Calcination: Disgregated fibers were heat treated at 120°C for 30 min to remove water and after that at 505°C for 1h to remove any organic substance, such as sizing or impurities. A thermocouple placed near the sample was used to control the temperature.
- ✓ Activation: The calcinated fibers were subjected to an activation process with commercial chlorhydric acid aqueous solution (37% wt) for 1h to regenerate silanol groups, Si-OH, on the fiber surface. After that, all samples were washed with destilled and deionized water and finally dried at 110°C for 1 h and stored in a dessicator until silanization.
- ✓ Silanization: The fibers were then chemically coated with the aminosilane coupling agents. 1g of basalt fibers was inmersed in 50 ml of silane 2% wt aqueous solution for 1h at room temperature. In order to obtain different molecular structures different silane aqueous solutions were used: i) γ-aminopropiltriethoxysilane (APTES); ii) γ-aminopropilmethyldiethoxysilane (APDES) and iii) a mixture of them wirh a composition of 50% by weight (APTES+APDES).

After squeezing the fibers, the adsorbed silane was cured at 110 °C for 1h to accelerate condensation reaction and to remove water. In order to eliminate some unreacted silane monomers or oligomers that could remain physisorbed on the basalt fibers surface the fibers were subjected to a Soxhlet extraction with dry toluene for 3 h. Finally, fibers were put in an oven at 110°C for 1h to remove adsorbed toluene [14,16,18,23,32].

As an aproximation the structures expected for the basalt fibers surfaces using the different silane solutions would be those shown in Figure 1 [23]: i) smooth surfaces with low concentration of silanol groups for calcinated basalt fibers; ii) smooth surfaces with increased concentration of surface silanols groups for activated fibers; iii) surfaces with lineal or bowed siloxane coating when APDES is used and iv) crosslinked siloxane structures when APTES solutions are used being higher the crosslinking degree the higher the APTES concentration.

Therfore when a mixture of silanes (APTES+APDES) is used a more open crosslinked structure is expected.

2.3 Experimental Techniques

2.3.1 X-Ray Diffraction (XRD)

Structural characteristics of as-received, calcinated and activated basalt fibers were studied by X-Ray Diffraction (XRD) using a Bruker AXS D8 ADVANCE diffractometer with a CuKα1 radiation, step size of 0.020°, time per step of 1 s from 5° to 65°.

2.3.2 Thermal analysis

Thermogravimetric analysis was carried out using a Mettler Toledo TGA/SDTA 851e analyzer equipped with a TSO800GC1 flow gas controller and a TSO801RO universal samples robot. The analysis of the as-received and treated basalt fibers were performed using a platinum crucible at 10°C/min heating rate under inert atmosphere from 30°C to 800°C.

2.3.3 *Fourier Transform Infrared Spectroscopy (FT-IR)*

FT-IR spectra of as-received and modified basalt fibers were recorded with a FT-IR Spectrum GX (Perkin-Elmer). Basalt fibers (as-received and treated) was ground, mixed with KBr powder and pressed using a Specac Press to make discs of 1 cm of diameter to perform the FTIR studies in the transmission mode. In particular, discs with 1% and 5% by weight of fibers were considered to better visualized absorption bands in the low and high energy regions of the spectra respectively. As background, a pure KBr disc was used. Every spectrum was recorded from 400 to 4000 cm^{-1} using 2 cm^{-1} of resolution and 20 scans for the corresponding interferogram averaging. Finally, taking into account the proportionality between absorbance and the amount of the absorbing species, to represent the spectra all of

them were normalized respect to the well weighted amount of fibers used to prepare the KBr discs.

2.3.4 Scanning electron microscopy (SEM)

As-received and treated basalt fibers were inspected by scanning electron microscopy using a TENEO field emission scanning electron microscope, FESEM (FEI). The acceleration voltage was 2.0 kV and the T1 detector was used taking the signal coming from backscattered electrons. As the samples are not conductive, prior to examination, they were sputter coated with gold using a low vacuum coater Leica EM ACE200.

2.3.5 Atomic force microscopy (AFM)

Atomic force microscopy, AFM, was used to inspect topographical characteristics of the basalt fibers. A microscope Multi-Mode Nanoscope IVA (Digital Instruments/Veeco Metrology Group) was used. All measurements were conducted at ambient conditions in tapping mode with antimony doped silicon probe (k = 1-5 N/m). The frequency was adjusted to the resonant frequency of the probe close to the surface of the sample to be analyzed. The initial amplitude of the probe oscillation and set-point amplitude applied for imaging were chosen to maximize the image contrast among the different constituents of the samples.

3. RESULTS AND DISCUSSIONS

3.1 Characterization of As-Received Basalt Fibers

In the Figure 2 XRD patterns of the as-received (a), calcinated (b) and activated (c) basalt fibers are shown. XRD analysis of the commercial basalt fibers reflects only an amorphous structure without any evidence of crystalline phases being in accordance with bibliography [33,34]. Besides, the either the calcination or the activation processes do not seem to change the structure of the basalt fibers at least in terms of cristallinity.

In Figure 3 TGA curves (top) and its corresponding derivatives DTGA (bottom) are shown for all the basalt fibers considered in the present work. In particular, for the as-received fibers, represented by the black curves, two clear observations can be made: the weight loss at about 100 ºC due to the adsorbed water on the fiber and a thermal degradation process in the range going from 200 to 550 °C with a weight loss of 0.4% by weight (Table 1). This degradation can be ascribed to the presence of the organic coating associated to the sizing of the commercial fibers. It is important to point out that around the temperature of 450 ºC the dehydroxilation process of silica occurs which involves the condensation of surface hydroxyl groups to form siloxane bonds releasing water molecules [24,35]. Therefore, the weight loss calculated in this range might include part of the water associated to this process. Nevertheless, this result points out that the conditions selected for the calcination process 505 ºC for 1 h should be enough to fully remove the commercial sizing avoiding simultaneously an excessive dehydroxilation of the surface.

The FT-IR spectrum of as-received basalt fiber is shown in the Figure 4. In the region of high energy the FTIR spectrum of the commercial basalt fibers (Figure 4a) shows a broad band from 3600-3200 cm^{-1} that usually is assigned to the hydrogen bonded O-H stretching that can come either from water adsorbed on the fiber surface or from the silanol groups, -Si-OH [32,36].

In the range from 3000 to 2800 cm^{-1} the characteristic CH stretching bands coming from the methylene, CH_2, and methyl, CH_3, groups can be observed. These bands ensured the organic character which is typical of the most common sizings used in the production process of glass and basalt fibers. In the low energy region of the spectrum (Figure 4b) the absorption bands at 1000 and 740 cm^{-1} corresponding to the Si-O vibrations typical of silane sizings and basalt fibers (they are mainly composed by SiO_2) are detected.

The morphology and topography of the as-received basalt fibers were studied by SEM and AFM (Fig. 5a and 5b). Dark grey in the SEM and light yellow "islands" in the AFM height images reflect a heterogeneous surface of the fibers due to the presence of the sizing. Moreover, some regions in the SEM image (pointed by an arrow) suggest that the shape of the fibers is not perfectly cylindrical but it presents some imperfections. These imperfections, similar to a valley on the fiber surface are also clearly visible in the 3D AFM images (Figure 5c) of treated basalt fibers.

3.2 Characterization of modified Basalt Fibers

XRD Analysis, Fig, 2b and 2c, shows that calcinated and activated basalt fibers are characterized by the same structure of as-received basalt fibers (Fig.2a). The amorphous structure of the as-received basalt fibers without any evidence of crystalline phases is preserved. It is possible to confirm that calcination and activation processes carried out in order to obtain an ideal surface necessary to apply the new chemical coatings based on aminosilanes, do not modify the structure of the original basalt fibers.

From the TGA and DTGA curves (Figure 3) the thermodegradation process associated to the organic matter was analyzed within the range 200°C - 400°C in order to be sure that only organic coating is analyzed avoiding to count for the water release due to the deshydroxylation phenomenon. The weight loss in every case was calculated and gathered in the Table 1.

As can be seen and attending the accuracy of the thermobalance the data in the Table 1 suggest that a treatment at 505 °C for 1 h is enough to remove the whole sizing of the commercial fibers. As it is shown, calcination process helps to completely remove the original sizing. On the other hand, DTGA curves show (Figure 3) that the maximum rate of thermodegradation for the aminosilane coatings are shifted to higher temperatures respect to that observed for the sizing of the as-received basalt fibers indicating, as expected, different

structures. Usually commercial sizings are formed by a mixture of several components, silanes, plasticizers, lubricants, etc. In Table 1 it can be seen that the order in terms of degree of coating is: APTES > APTES+APDES > APDES, as expected if higher functionality implies higher reactivity with higher amount of monomer incorporation. It is observed that the silane with a crosslinked structure is grafted in more amount on the fiber surface than the silane with a linear structure.

FTIR was also used to study structural variation of the basalt fiber surface with the different treatments considered. In the Figure 4 FTIR the spectra of all the modified or unmodified basalt fibers are represented. Paying attention to the high energy region (Figure 4a) some clear observations can be made: a) after calcination there is a reduction of the broad band centered at about 3450 cm^{-1} that can be mainly associated to a decrease in the adsorbed water since no clear evidence of deshydroxilation at 505 ºC was observed by TGA (Figure 3). Besides, b) the absorption bands due to CH (CH_2, CH_3) stretching vibrations of the sizing disappear. c) When the activation process is carried out an increase of the band at 3450 cm^{-1} occurs evidencing the existence of higher number of hydrogen bonded OH probably coming from more adsorbed water induced by a more hydrophilic surface with higher silanol groups content. In fact, the reason why the HCl treatment was called activation is because a more reactive surface is created by means of a silanol groups regeneration as it was explained elsewhere [32,37]. Taking into account several reported assignations of absorption bands (see Table 2) [38], an easier analysis of the silane coated fibers FTIR spectra can be done.

It is clear therefore that the presence of aminosilanes can be identified with absorption bands at 3400-3300 cm^{-1} due to N-H stretching modes. On the other hand, in the range of 3000-2800 cm^{-1} the C-H stretching bands arising from the methylene, CH_2, and methyl, CH_3, groups are observed. In fact, as expected from the chemical structures of the hydrolyzed silanes used (Figure 6), only for the APTES coating the band at 2960 cm^{-1} does not appear which indicates the absence of methyl groups.

Finally, from the FTIR results an estimation of the amount of silane grafted on the fibers surface was carried out. The amount of silane showing in the Table 3 was calculate from the measurement of absorbance of the band at 2930 cm^{-1} corresponding to the CH stretching band of the CH_2 group using the following equation:

$$c = A_{2930}/3Kb \qquad (1)$$

where **c** is the silane concentration in mol/cm^3, $\boldsymbol{A_{2930}}$ is the absorbance corresponding to the CH absorption band of the CH_2 group, $\boldsymbol{K}$ is the specific absorptivity for the silane (1.7 x 10^4 cm^2/mol) and $\boldsymbol{b}$ is the optical path. Division by 3 is performed to take into account the three methyl groups contribution of each molecule hydrolyzed silane [38,39]. An estimation of the amount of silane in terms of percentage was at the same time carried out. Taking into account the volume of discs and the silane concentration in mol/cm^3 previously calculated according the equation mentioned above, the moles number of the CH_2 group present in each disc and thus the moles number of each silane were calculated. In this way considering the molecular weight of each silane used, the silane weight in the disc was obtained. In the case of the mixture of the two silanes, an average of the molecular weight was considered. Finally, knowing the initial weight of the discs (including fiber and silane weights), the percentage respectively of each silane was obtained. The results are shown in the Table 3.

According to TGA results, it is observed that the silane content seems to follow the order: APTES > APTES+APTES > APDES. The small differences found between the results provided by the two techniques could be ascribed to the associated error to the measuring instruments.

Although relevant results are obtained from the high energy region of the spectra, not significant observations can be drawn from the low energy region of FTIR spectra.

In Figure 7, the SEM images of treated basalt fibers compared to as-received basalt fibers are shown. Calcinated (b) and activated (c) basalt fibers look very similar each other;

nevertheless, some differences due to the processes are better observed by AFM analysis (Figure 8). However, as a consequence of these two treatments a smoother surface due to the removal of original sizing can be observed.

Finally, the images (d, e, f) of Figure 7, corresponds to the silanized basalt fibers after the heat cleaning and activation processes. As a result of the incorporation of the aminosilanes, some heterogeneities are observed on the fibers surfaces. In particular, these heterogeneities are more clear when the APTES, the aminosilane with a crosslinked structure, is applied.

Changes on the fibers surface are better studied by AFM because the preliminary preparation of the sample to be analyzed is quite easy. Besides, the gold coating used to observe samples by SEM might hide some small superficial characteristics.

In the Figure 8, 3D AFM images of the as-received and treated basalt fibers are shown.

A kind of "islands" are better observed on the commercial fiber surface arising from the sizing (Figure 8a). The images corresponding to the calcinated basalt fibers (Figure 8b) shows sometimes a kind of scratches which might reflect locations where fibers could be joined by the action of the sizing. However, the amount of remaining sizing is almost zero because no evidence of organic coating was detected by FTIR spectroscopy and only a small amount of organic substance (weight loss of 0,04%) was detected by TGA that might be considered negligible. On the other hand, according to TGA results shown in the Table 1 and the observations of 3D AFM images like in Figure 8c it is evidenced that the activation process ensures total removal of those possible amounts of remaining sizing making the fiber surface clearly smoother.

In comparison with the SEM images, the 3D AFM images of the silanized basalt fibers (Figures 8d and 5c) better show the heterogeneous topography given by the coating. It can be observed that the distribution of the coupling agents on the fibers is in the form of droplets; i.e. there is formation of islands on the fiber being in accordance with other results the scientific literature observed for E-glass fibers treated with aminosilanes [19]. Furthermore, it

is interesting to highlight that the way of coating depends on the kind of silane used. The islands of sizing seem to be homogeneously distributed on the basalt fiber surface when they are treated with *γ-aminopropilmethyldiethoxysilane* (APDES) whereas "mountains-like" of sizing are better observed when the *γ-aminopropiltriethoxysilane* (APTES) is used. These observations suggest that topography due to the heterogeneities arising from the sizing deposition could be controlled and therefore parameters as the roughness which are essential to finally attain good adherence or interface properties when the fibers are use as reinforcements in composites.

4. CONCLUSIONS

Surface treatments and subsequent characterization of basalt fibers were carried out in this work. the preliminary study about the structure, composition and morphology/topography of as-received basalt fibers by several analytical techniques (XRD, TGA, FT-IR, FE-SEM and AFM) confirmed that commercial fibers are characterized by an amorphous structure and a heterogeneous sizing of organic nature applied on the fiber surface during the production process;

- Depending on the treatment given changes in the structure, composition and topography are observed. In particular, the calcination process removes the most of commercial sizing present on the fiber surface making the surface smooth.
- The activation process fully removes all residues of sizing that could remain on the calcinated fiber surface and makes the topography smoother than calcination process. Moreover, this process regenerate silanol groups on the fiber surface allowing the grafting of aminosilanes.
- The three chemical coatings based on aminosilane (APTES, APDES and APTES+APDES) make the surface rough. It was concluded that the higher the amount of triethoxysilane in the composition of the coating solution, the more organic matter deposited

on the fibers, so as the topographical heterogeneity. This heterogeneity could be responsible of a most adhesion between the matrix and the fiber.

REFERENCES

[1] K. Singha, A Short Review on Basalt Fiber, Int. J. Text. Sci. 1 (2012) 19–28. doi:10.5923/j.textile.20120104.02.

[2] V. Fiore, T. Scalici, G. Di Bella, A. Valenza, A review on basalt fibre and its composites, Compos. Part B Eng. 74 (2015) 74–94. doi:10.1016/j.compositesb.2014.12.034.

[3] J. Militký, V. Kovačič, J. Rubnerová, Influence of thermal treatment on tensile failure of basalt fibers, Eng. Fract. Mech. 69 (2002) 1025–1033. doi:10.1016/S0013-7944(01)00119-9.

[4] V. Manikandan, J.T. Winowlin Jappes, S.M. Suresh Kumar, P. Amuthakkannan, Investigation of the effect of surface modifications on the mechanical properties of basalt fibre reinforced polymer composites, Compos. Part B Eng. 43 (2012) 812–818. doi:10.1016/j.compositesb.2011.11.009.

[5] V. Dhand, G. Mittal, K.Y. Rhee, S.-J. Park, D. Hui, A short review on basalt fiber reinforced polymer composites, Compos. Part B. 73 (2015) 166–180. doi:10.1016/j.compositesb.2014.12.011.

[6] J. Sim, C. Park, D.Y. Moon, Characteristics of basalt fiber as a strengthening material for concrete structures, Compos. Part B Eng. 36 (2005) 504–512. doi:10.1016/j.compositesb.2005.02.002.

[7] B. Wei, S. Song, H. Cao, Strengthening of basalt fibers with nano-SiO2-epoxy composite coating, Mater. Des. 32 (2011) 4180–4186. doi:10.1016/j.matdes.2011.04.041.

[8] G. Quattrociocchi, M. Albé, J. Tirilló, F. Sarasini, M. Valente, M.L. Santarelli, Basalt fibres as a sustainable reinforcement for cement based mortars: preliminary study, 90 (2015) 109–120. doi:10.2495/MC150101.

[9] M.L. Santarelli, F. Sbardella, M. Zuena, M. Albé, G. Quattrociocchi, J. Tirilló, M. Valente, F. Sarasini, Malte più performanti con le fibre di basalto, Compos. Mag. 33 (2014) 7–16. http://hdl.handle.net/10278/44412.

[10] M.L. Santarelli, F. Sbardella, M. Zuena, J. Tirillò, F. Sarasini, Basalt fiber reinforced natural hydraulic lime mortars: A potential bio-based material for restoration, Mater. Des. 63 (2014) 398–406. doi:10.1016/j.matdes.2014.06.041.

[11] N. Suzuki, H. Ishida, A Review on the Structure and Characterization Techniques of Silane/Matrix Interphases, 108 (1096) 19–53.

[12] A.T. DiBenedetto, Evaluation of fiber surface treatments in composite materials, Pure Appl. Chem. 57 (1985) 1659–1665. doi:10.1351/pac198557111659.

[13] V.A. Rybin, A. V. Utkin, N.I. Baklanova, Alkali resistance, microstructural and mechanical performance of zirconia-coated basalt fibers, Cem. Concr. Res. 53 (2013) 1–8. doi:10.1016/j.cemconres.2013.06.002.

[14] J.G. Iglesias, J. González-Benito, A.J. Aznar, J. Bravo, J. Baselga, Effect of Glass Fiber Surface Treatments on Mechanical Strength of Epoxy Based Composite Materials, J. Colloid Interface Sci. 250 (2002) 251–260. doi:10.1006.

[15] S.-J. Park, J.-S. Jin, J.-R. Lee, Influence of silane coupling agents on the surface energetics of glass fibers and mechanical interfacial properties of glass fiber-reinforced composites, J. Adhes. Sci. Technol. 14 (2000) 1677–1689. doi:10.1163/156856100742483.

[16] D. Olmos, J. González-Benito, Visualization of the morphology at the interphase of glass fibre reinforced epoxy-thermoplastic polymer composites, Eur. Polym. J. 43 (2007) 1487–1500. doi:10.1016/j.eurpolymj.2007.01.004.

[17] D. Olmos, R. López-Morón, J. González-Benito, The nature of the glass fibre surface and its effect in the water absorption of glass fibre/epoxy composites. The use of fluorescence to obtain information at the interface, Compos. Sci. Technol. 66 (2006) 2758–2768. doi:10.1016/j.compscitech.2006.03.004.

[18] J. González-Benito, A. Aznar, J. Baselga, Solvent and Temperature Effects on Polymer-Coated Glass Fibers . Fluorescence of the Dansyl Moiety, J. Fluoresc. 11 (2001).

[19] S.G. Turrión, D. Olmos, J. González-Benito, Complementary characterization by fluorescence and AFM of polyaminosiloxane glass fibers coatings, Polym. Test. 24 (2005) 301–308. doi:10.1016/j.polymertesting.2004.11.006.

[20] J. González-Benito, The nature of the structural gradient in epoxy curing at a glass fiber/epoxy matrix interface using FTIR imaging, J. Colloid Interface Sci. 267 (2003) 326–332. doi:10.1016/S0021-9797(03)00550-2.

[21] D. Olmos, A.J. Aznar, J. Baselga, J. González-Benito, Kinetic study of epoxy curing in the glass fiber/epoxy interface using dansyl fluorescence, J. Colloid Interface Sci. 267

(2003) 117–126. doi:10.1016/S0021-9797(03)00620-9.

[22] E. Metwalli, D. Haines, O. Becker, S. Conzone, C.G. Pantano, Surface characterizations of mono-, di-, and tri-aminosilane treated glass substrates, J. Colloid Interface Sci. 298 (2006) 825–831. doi:10.1016/j.jcis.2006.03.045.

[23] D. Olmos, J. Gonzalez-Benito, Composites formed by glass fibers and PS-modified epoxy matrix. Influence of the glass fibers surface on the morphologies and mechanical properties of the interphases generated, Polym. Compos. 31 (2010) 946–955. doi:10.1002/pc.20879.

[24] M. Jiménez, J. González-Benito, A.J. Aznar, J. Baselga, Degradación hidrolítica de recubrimientos polisiloxánicos de fibras de vidrio, 39 [4] (2000) 425–430.

[25] R.B. J.M. España, M.D. Samper, E. Fages, L. Sanchez-Nacher, Investigation of the Effect of Different Silane Coupling Agents on Mechanical Performance of Basalt Fiber Composite Laminates with Biobased Epoxy Matrices J.M., Polym. Compos. 34 (2013) 376–381. doi:10.1002/pc.

[26] T. Deák, T. Czigány, P. Tamás, C. Németh, Enhancement of interfacial properties of basalt fiber reinforced nylon 6 matrix composites with silane coupling agents, Express Polym. Lett. 4 (2010) 590–598. doi:10.3144/expresspolymlett.2010.74.

[27] Y. Xie, C.A.S. Hill, Z. Xiao, H. Militz, C. Mai, Silane coupling agents used for natural fiber/polymer composites: A review, Compos. Part A Appl. Sci. Manuf. 41 (2010) 806–819. doi:10.1016/j.compositesa.2010.03.005.

[28] E. Feresenbet, D. Raghavan, G.A. Holmes, The influence of silane coupling agent composition on the surface characterization of fiber and on fiber-matrix interfacial shear strength, J. Adhes. 79 (2003) 643–665. doi:10.1080/00218460309580.

[29] B. Wei, H. Cao, S. Song, Surface modification and characterization of basalt fibers with hybrid sizings, Compos. Part A Appl. Sci. Manuf. 42 (2011) 22–29. doi:10.1016/j.compositesa.2010.09.010.

[30] P. Hosseini, R. Hosseinpourpia, A. Pajum, M.M. Khodavirdi, H. Izadi, A. Vaezi, Effect of nano-particles and aminosilane interaction on the performances of cement-based composites: An experimental study, Constr. Build. Mater. 66 (2014) 113–124. doi:10.1016/j.conbuildmat.2014.05.047.

[31] F. Švegl, J. Šuput-Strupi, L. Škrlep, K. Kalcher, The influence of aminosilanes on macroscopic properties of cement paste, Cem. Concr. Res. 38 (2008) 945–954.

doi:10.1016/j.cemconres.2008.02.006.

[32] J. González-Benito, J. Baselga, A.J. Aznar, Microstructural and wettability study of surface pretreated glass fibres, J. Mater. Process. Technol. 92–93 (1999) 129–134. doi:10.1016/S0924-0136(99)00212-5.

[33] M. Welter, M. Schmücker, K.J.D. MacKenzie, Evolution of the fibre-matrix interactions in basalt-fibre-reinforced geopolymer-matrix composites after heating, J. Ceram. Sci. Technol. 6 (2015) 17–24. doi:10.4416/JCST2014-00034.

[34] S.I. Gutnikov, M.S. Manylov, Y. V. Lipatov, B.I. Lazoryak, K. V. Pokholok, Effect of the reduction treatment on the basalt continuous fiber crystallization properties, J. Non. Cryst. Solids. 368 (2013) 45–50. doi:10.1016/j.jnoncrysol.2013.03.007.

[35] L.T. Zhuravlev, The surface chemistry of amorphous silica. Zhuravlev model, Colloids Surfaces A Physicochem. Eng. Asp. 173 (2000) 1–38. doi:10.1016/S0927-7757(00)00556-2.

[36] J. Gonzalez-Benito, J.C. Cabanelas, a J. Aznar, M.R. Vigil, J. Bravo, J. Baselga, Surface characterization of silanized glass fibers by labeling with environmentally sensitive fluorophores, J. Appl. Polym. Sci. 62 (1996) 375–384. doi:10.1002/(SICI)1097-4628(19961010)62:2<375::AID-APP12>3.3.CO;2-V.

[37] A.Larena, J.Martínez Urreaga, M.U. de la Orden, Effects of previous leaching with hydrochloric acid of E-glass short fibre on the fibre reaction with chlorosilanes, Mater. Lett. 12 (1992) 415–418.

[38] D. Olmos Díaz, Materiales compuestos epoxi-sílice: estudio de interfases, (2003) 247. http://hdl.handle.net/10016/11351.

[39] C.-H. Chiang, H. Ishida, J.L. Koenig, The structure of γ-aminopropyltriethoxysilane on glass surfaces, J. Colloid Interface Sci. 74 (1980) 396–404. doi:10.1016/0021-9797(80)90209-X.

Table 1. TGA results of as-received and treated basalt fibers

Sample	*Temperature Range (ºC)*	*Weight loss (%)*
AS-RECEIVED	200 - 550	0,40
AS-RECEIVED	200 - 400	0,28
CALCINATED	200 - 400	0,04
ACTIVATED	200 - 400	0,02
APTES	200 - 400	0,21
APTES+APDES	200 - 400	0,19
APDES	200 - 400	0,03

Table 2. Absorption Bands of Aminosilanes [38].

ν (cm^{-1})	***Absorption bands of Aminosilane***
3400	ν (O-H)
3400-3300	ν_{as} (N-H)
2970-2960	ν_{as} (C-H) (CH_3)
2930-2920	ν_{as} (C-H) (CH_2)
1600	δ (N-H)
1450	δ (CH_2)
1440	δ (CH_3)
1410	δ (Si- CH_2)
1380	δ (CH_3)
1260	ν (Si-C)
1160	ρ (CH_3)
1100	ν_{as} (Si-OSi)
1100	ν_{as} (Si-OC)
1000	ν_{as} (Si-OSi)
950	δ (Si-OH)

Table 3. Estimation of the concentration of silane on the fiber surface by FTIR

Sample	A_{2930}	*b (cm)*	*c (mol/cm^3)*	*% weight by FTIR*	*% weight by TGA**
APTES	0,029	0,0451	$1{,}26 \times 10^{-5}$	0,30	0,21
APTES+APDES	0,023	0,0453	$9{,}95 \times 10^{-6}$	0,23	0,19
APDES	0,017	0,0512	$6{,}51 \times 10^{-6}$	0,17	0,03

* Table 1

Figure
Click here to download Figure: FIGURES.docx

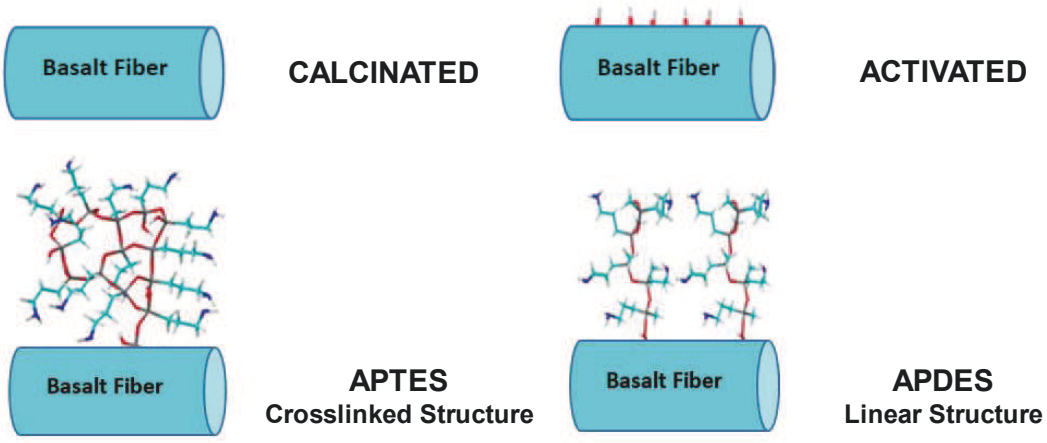

Figure 1

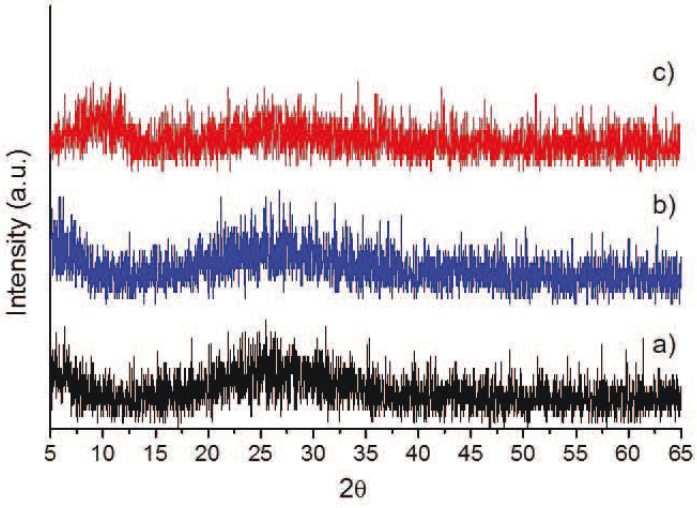

Figure 2

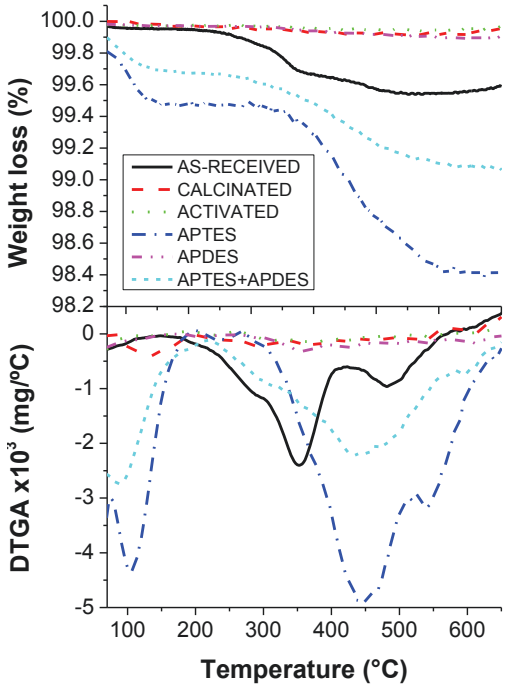
Weight loss (%)
100.0
99.8
99.6
99.4
99.2
99.0
98.8
98.6
98.4
98.2
AS-RECEIVED
CALCINATED
ACTIVATED
APTES
APDES
APTES+APDES
DTGA x10³ (mg/°C)
0
-1
-2
-3
-4
-5
100
200
300
400
500
600
Temperature (°C)

Figure 3

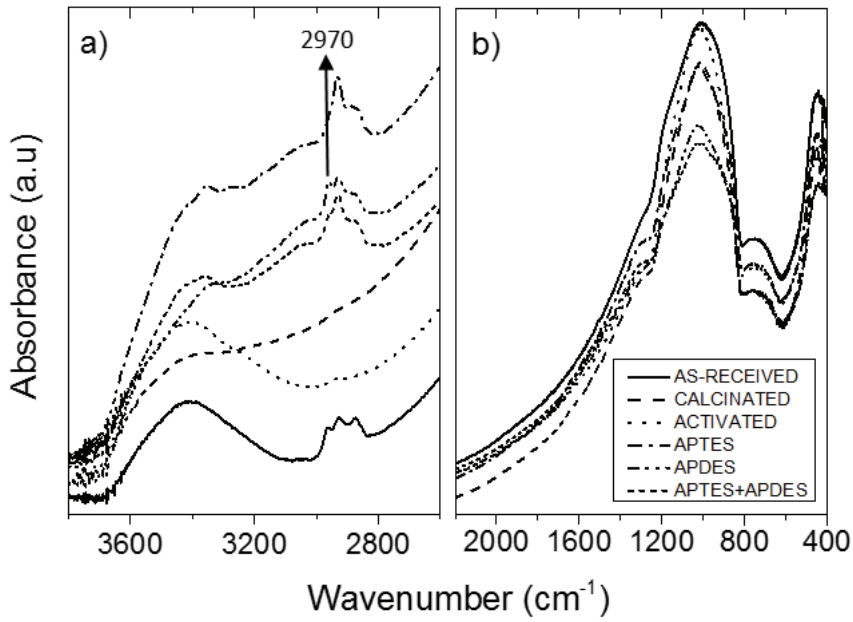
a)
2970
b)
Absorbance (a.u)
AS-RECEIVED
CALCINATED
ACTIVATED
APTES
APDES
APTES+APDES
3600
3200
2800
2000
1600
1200
800
400
Wavenumber (cm-1)

Figure 4

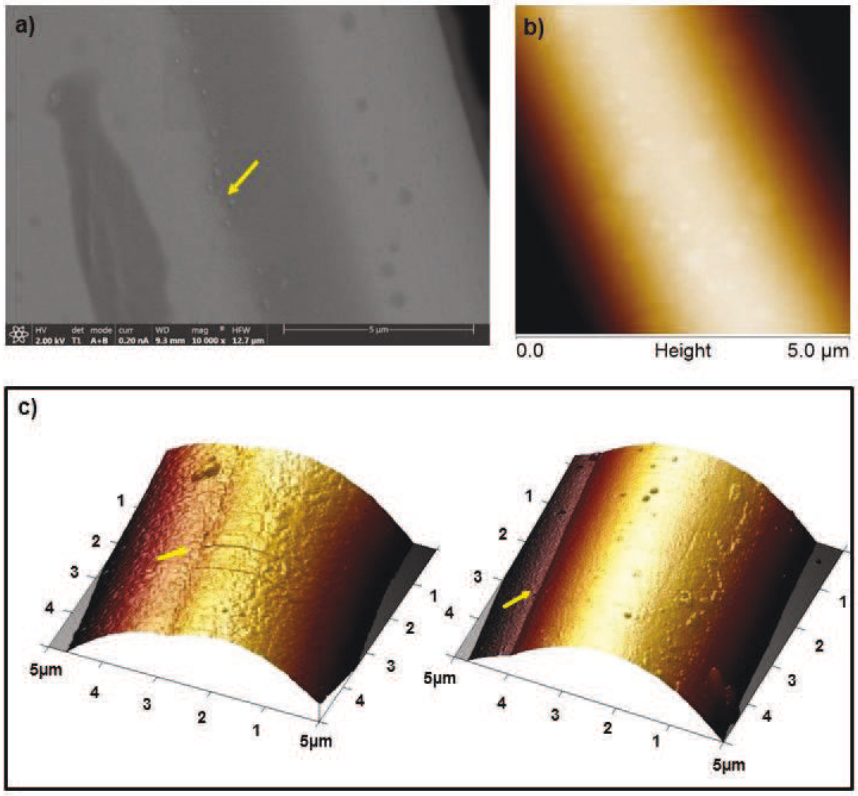

Figure 5

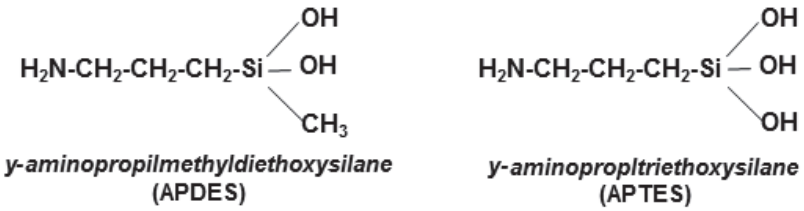

y-aminopropilmethyldiethoxysilane
(APDES)

y-aminopropltriethoxysilane
(APTES)

Figure 6

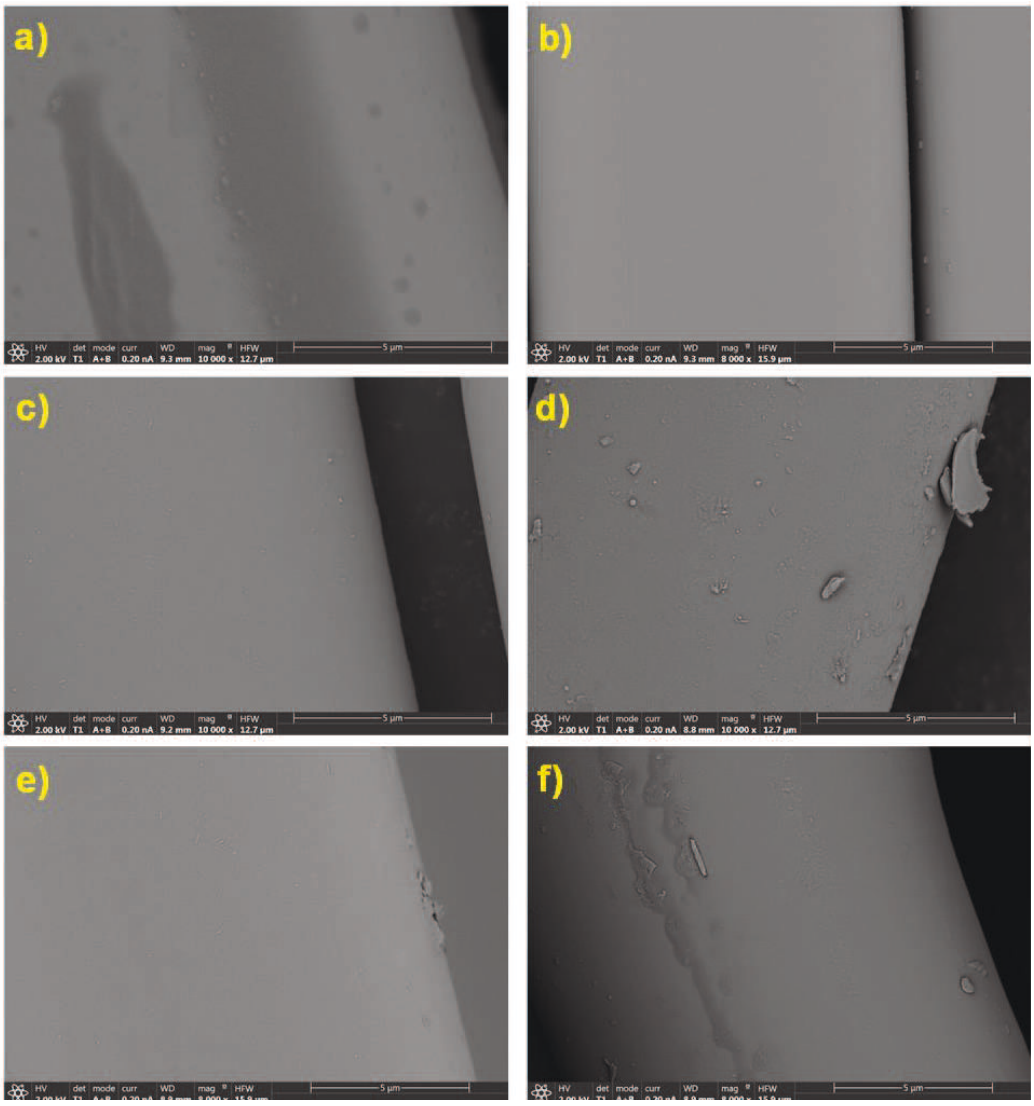

Figure 7

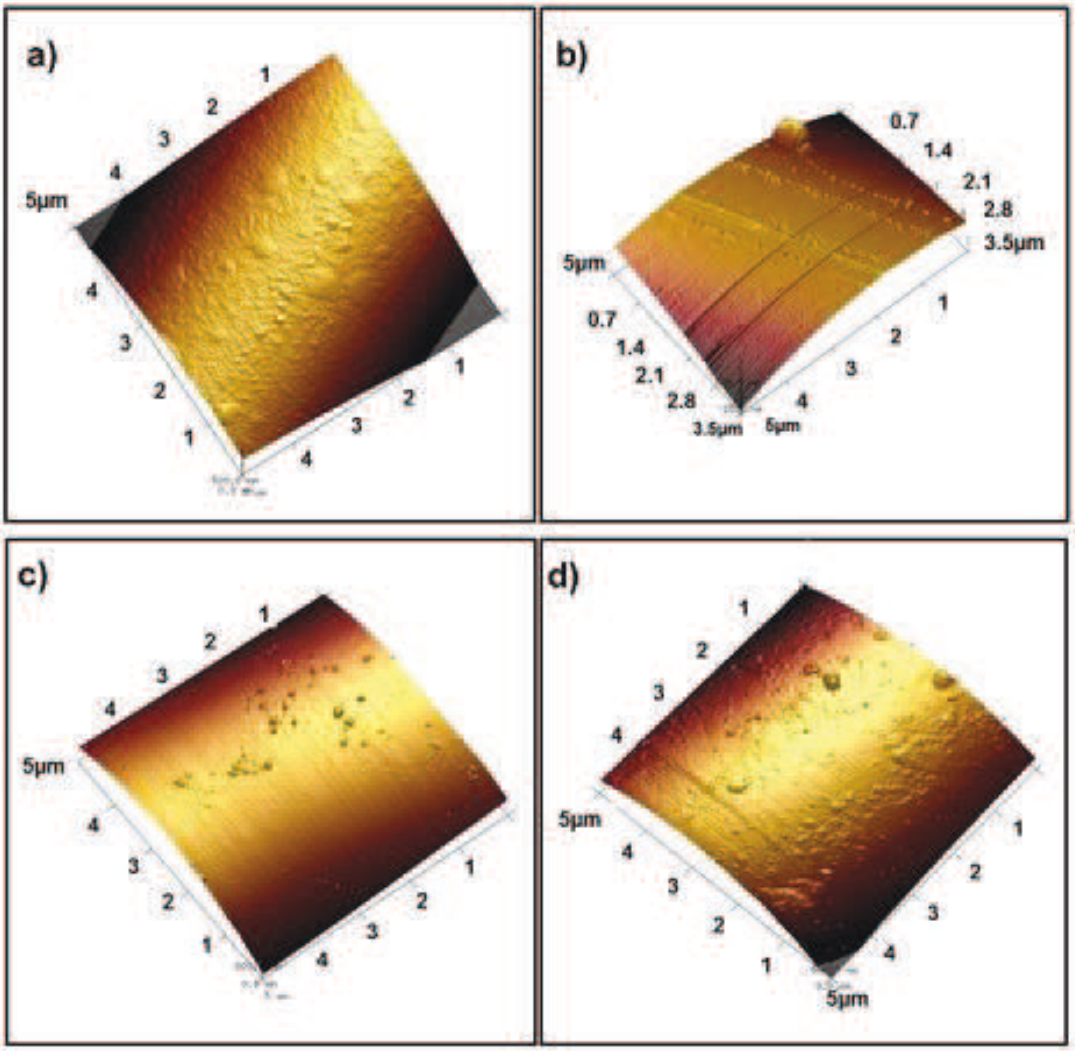

Figure 8

LIST OF FIGURE CAPTIONS

Click here to download Supplementary Material for on-line publication only: LIST OF FIGURE CAPTIONS.docx